SAE International

2013-01-1532
Published 04/08/2013

doi:10.4271/2013-01-1532
saealtpow.saejournals.org

Lead-Acid State of Charge Estimation for Start-Stop Applications

Daniel Le and Brian Sisk
Johnson Controls Power Solutions

ABSTRACT

Start-stop, aka engine-stop or idle-stop, technologies are increasingly being applied to automotive vehicles to increase fuel economy. Start-stop vehicles turn off the engine during periods of zero speed and/or during prolonged coast down. During engine-stop, the vehicle electronics are powered solely by the battery. To replenish the battery, the battery needs to be recharged. In typical ICE vehicles, the battery is continuously charged. However, fuel economies can be improved if strategic charging of the battery can be achieved through selective charging through the alternator or through regenerative braking. To optimize fuel economy, an accurate estimation of the battery state of charge (SOC) during vehicle operation is required. Although state of charge estimation has mainly focused on Li-ion batteries, lead-acid batteries may be used successfully in start-stop applications. However, SOC estimation for lead-acid batteries is particularly difficult due to side reactions and losses during charging, particularly at high SOC. This is a highly nonlinear function and requires special attention. To estimate the battery SOC, an equivalent-circuit lead-acid battery model is used to simulate the battery dynamics. This model incorporates losses associated with top charging which can affect the battery SOC estimation. In addition, parameter estimation techniques are utilized to identify the dynamic model parameters. Through this research, an online adaptive battery model can be used to estimate the lead-acid battery state of charge for start-stop applications, where the charging patterns may affect the SOC estimation.

CITATION: Le, D. and Sisk, B., "Lead-Acid State of Charge Estimation for Start-Stop Applications," *SAE Int. J. Alt. Power.* 2(1):2013, doi:10.4271/2013-01-1532.

INTRODUCTION

Traditional use of the lead-acid battery has been limited to SLI (Starting Lighting Ignition) functions. In addition, the alternator is continuously run to maintain battery state of charge (SOC) near 100% and the battery is constrained to a very shallow depth of discharge (DoD). However, with increasing vehicle electrification and efforts to improve the vehicle fuel efficiency, new requirements and accessory loads will significantly increase demands on the 12V battery.

In addition to traditional SLI functions, the battery must be able to provide and stabilize the electrical load required for additional electronics in the vehicle. This can include Bluetooth, GPS, DVD, Radio, etc which all utilize electrical energy supplied by the alternator and battery. Also, the battery has taken on additional functions to improve the vehicle fuel economy.

Specifically, in start-stop applications, the battery is used to maintain vehicle electronics during vehicle stop and then is used to restart the engine. This helps to reduce fuel consumption during idle. The battery can also be used to support vehicle electronics during passive boost operation. In this mode, the alternator is turned off so that the total engine power is applied to traction. During passive boost, the battery continues to supply electrical energy to the vehicle. Additionally, the battery can improve fuel economy by recovering brake energy. Coupled to a generator, the negative torque generated from braking or coast-down events can be used to slow down the vehicle and generate electrical energy which can be stored in the battery. This energy offsets the energy that would have been supplied through the alternator and further reduces the vehicle's fuel consumption. These additional battery functions require improved battery performance and monitoring to ensure proper battery operation, life, and safety.

In this paper, a battery model and algorithm are developed to simulate the battery dynamics under charge and discharge within a start-stop vehicle. The model and algorithm work to provide critical battery information such as battery state of charge. The remainder of this paper will describe the lead-acid battery model, the algorithm used to estimate the battery SOC, and examples of SOC estimation from a Federal Test Protocol (FTP-75) drive cycle for a start-stop vehicle.

EXPERIMENTAL SETUP

Battery Dynamics and Modeling

Lead-acid batteries are relatively simple in design but involve complex dynamics. The battery design is composed of an anode, cathode, separator, and electrolyte. At full charge, the anode is composed of lead, Pb, while the cathode is composed of lead dioxide, PbO_2, as seen in Figure 1(a). Under discharge, the anode and cathode undergo chemical reactions to produce $PbSO_4$ and, most importantly, free electrons which are able to produce electrical energy. At full discharge, the anode and cathode become $PbSO_4$, as seen in Figure 1(b). During charging, external electrical energy converts the $PbSO_4$ back into Pb and PbO_2 in the anode and cathode, respectively. The reactions are described below.

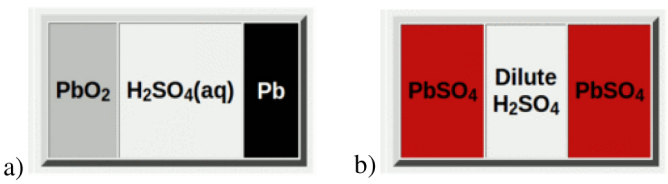

Figure 1. Anode and cathode composition under a) fully charged and b) fully discharged conditions.

Under discharge:
Negative plate reaction:

$$Pb(s) + HSO_4^-(aq) \rightarrow PbSO_4(s) + H^+(aq) + 2e^-$$

Positive plate reaction:

$$PbO_2(s) + HSO_4^-(aq) + 3H^+(aq) + 2e^- \rightarrow PbSO_4(s) + 2H_2O(l)$$

Under Charge:
Negative plate reaction:

$$PbSO_4(s) + H+(aq) + 2e^- \rightarrow Pb(s) + HSO_4^-(aq)$$

Positive plate reaction:

$$PbSO_4(s) + 2H_2O(l) \rightarrow PbO_2(s) + HSO_4^-(aq) + 3H^+(aq) + 2e^-$$

Ideally, all the reactions above would occur and there would be 100% Coulombic efficiency, in which all the electrons would participate and perform useful work in the process. However, in practice, this is not the case. There are side reactions, inefficiencies, and nonlinear dynamics that are associated with the battery charge and discharge. Although the bulk electrical characteristics are observable during charge and discharge, understanding and simulating the battery dynamics can be fairly complex.

Computational simulation of the battery is conducted by generating a representative model of the battery dynamics. There are 3 general classifications of battery models: 1) Heuristic Model, 2) Electro-chemical Model, and 3) Equivalent Circuit Model. Heuristic models are data-based models which fit a mathematical model to a dataset. These models are not usually based on fundamental physics but can provide an efficient method to simulate battery dynamics within specific operation limits. Electro-chemical models utilize the fundamental chemical reactions to determine battery dynamics. These models utilize the governing equations which describe the reactions, reaction rates, species conservation, etc. Electro-chemical models are computationally intensive but can provide very accurate results. Equivalent circuit models provide an intermediate model which utilizes the bulk properties of the battery to simulate the battery dynamics. Equivalent circuit models provide a valuable tradeoff in terms of functionality and accuracy. Equivalent circuit models apply real battery data and simulate the battery based on fundamental dynamics but avoids the tightly coupled multi-dimensional analysis associated with electrochemical models.

From an electrical perspective, the battery can be represented as an electrical device with a source, resistances, and capacitance. Linear and nonlinear battery dynamics such as Ohmic polarization, charge-transfer, diffusion, etc can be represented by combinations of capacitors and resistance in series/parallel configurations. In addition, side reactions, such as gassing, can be captured represented in this model.

In lead-acid battery models [1, 2, 3, 4, 5, 6], gassing reactions need to be represented. Gassing reactions refer to the electrolysis of water during charging. Under charge, near high SOC, lead-acid batteries experience gassing reactions which involve the dissociation of water molecules which reduces the Coulombic efficiency of the battery. Figure 2 shows the gassing reaction where water molecules split to form hydrogen gas in the cathode and oxygen in the anode. These reactions consume electrons, which would otherwise be used to charge the battery, and reduces the Coulombic efficiency.

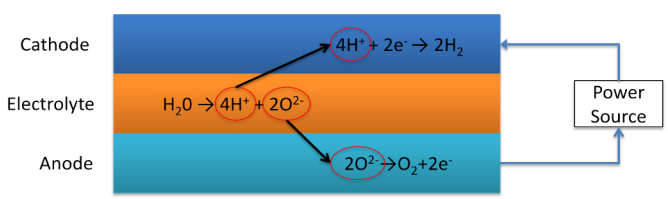

Figure 2. Water electrolysis under charging conditions.

This is particularly important since lead-acid batteries are typically top-charged to reach full SOC [7]. When the battery is top-charged, the gassing reaction increases with SOC. After 100% SOC, all of the energy goes towards the gassing reaction and the Coulombic efficiency reduces to zero. For vehicle fuel economy, this represents wasted energy. The gassing reaction rate also is dependent on the charging voltage. Typically lead-acid batteries begin gassing at ~2.35V/cell or 14.1V. Charging at voltages higher than this will increase the gassing reaction rate. In addition, oxygen evolution contributes to the corrosion of the anode.

Therefore, it is important to represent the gassing reactions to have more accurate estimates of the battery SOC and control side reactions.

One method to relate the gassing current to the voltage is through an expression similar to the Tafel equation. The Tafel equation relates the rate of electrochemical reactions to the voltage. This provides an expression that can relate the battery current and voltage based on fundamental reaction rates, as shown in Eq. (1). Equation (2) is based on the Tafel and used in this work to calculate the gassing current.

$$i = \eta F k exp\left(\alpha \eta F \, {\Delta V}/{RT}\right) \tag{1}$$

$$I_g = V_g \, G_{p0} exp\left({V_g}/{V_{g0}} + A_g\left(1 - {\theta}/{\theta_f}\right) \right) \tag{2}$$

The model used in this work incorporates linear and nonlinear electrical components to characterize the battery dynamics, as shown in Figure 3. The open-circuit voltage, OCV, is represented by a voltage source. The bulk resistances are captured by the linear resistance component. The nonlinear dynamics such as charge-transfer, double layer capacitance, and diffusion dynamics are lumped together using an RC component. Improvements to this model can separate the diffusion dynamics using a separate component. This would allow the time constants associated with each dynamic to be better represented. For simplicity, the nonlinear dynamics are lumped together and with a combined time constant. This is justified since it will still allow separation between linear and nonlinear dynamics in the system. Since the primary objective is to determine the battery SOC/OCV, this model will be sufficient. The gassing branch, V_g, simulates the losses associated with the gassing reactions. The charging current to the battery is split between the gassing branch, I_g, and the main branch, I_m. The relationship of main and gassing current to the terminal current, I, is given in Eq. (3). The losses due to gassing increases if the charging voltage is near or above the gassing voltage and if the battery SOC is very high. The battery terminal voltage is given by (4). The time-discrete representation of the RC voltage is given by (5). This model provides an efficient method to simulate the battery while incorporating sufficient details for accuracy.

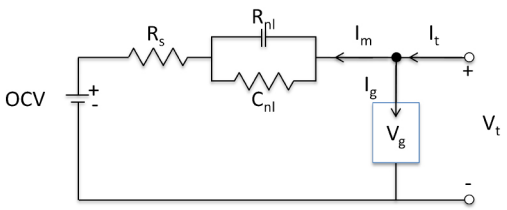

Figure 3. Lead-acid equivalent circuit model.

$$I = I_m + I_g \tag{3}$$

$$V(k) = OCV(k) + I_m(k)R_s(k) + V_1(k) \tag{4}$$

$$V_1(k) = V_1(k-1)\exp\left(-{dt}/{R_1C_1}\right) + R_1\left[1 - \exp\left(-{dt}/{R_1C_1}\right)\right] I_m(k-1) \tag{5}$$

Battery States and Parameters

Although battery models may capture the relative dynamics of the battery, the parameters and internal states of the battery vary dynamically. For example, the battery capacity varies with the battery load. Depending on the charge and discharge rates, the battery capacity will vary due to the limitations of the dissolution and precipitation processes. To give another example, the internal resistance is dependent on temp and SOC. At lower temperatures, the mobility of the ions throughout the material is lowered which results in a higher impedance values. The internal resistance is also a function of the battery SOC. As the battery is discharged to lower SOC levels, large lead-sulfate crystals form and increase the internal resistance of the battery. With limited sensing capabilities of the battery, advanced estimation and control algorithms are required to monitor and control the battery states.

State of charge and state of health (SOH) are important metrics which identify critical battery states. Battery SOC refers to the remaining charge available in the battery relative to the battery capacity. Battery SOH refers to the ability of the battery to safely and reliably store and deliver energy.

State of charge

Proper monitoring of the battery states has a direct implication on the battery performance, safety, and life. Battery SOC has direct implications on the battery regeneration and discharge ability. If the battery SOC is too low, the battery power may not be sufficient to provide the electrical power needed to sustain cranking capabilities, support boost, or maintain the electrical load for devices in the vehicle. However, if the battery SOC is too high, energy from regenerative braking will not be fully captured. It is important to maintain the proper operational SOC required for vehicle operation and optimize vehicle fuel efficiency. A simple method to calculate battery SOC is given by Eq. (6), commonly referred to as Coulomb counting.

$$SOC = SOC_o + \eta \int {Idt}/{Capacity} \tag{6}$$

However, even with such a simple equation, there are significant sources of error that can contribute to SOC error. If current integration is used to estimate SOC, non-Gaussian

noise in the current signal will contribute to SOC drift over time. This is magnified under top-charging conditions due to losses associated with the gassing reactions. Under charging, the Coulobmic efficiency decreases as the SOC increases. Also, the battery capacity is not exactly known, varies with operating conditions, and affects battery SOC calculations Any error in the battery capacity value will increase the SOC error. Also, nonlinear dynamics, such as diffusion, and losses in the battery due to internal resistances will also contribute to SOC error. Although it may be unrealistic to have exact SOC estimation during vehicle operation, it is important to maintain the SOC estimation accuracy within tolerable limits.

State of health

Battery SOH serves as an indication of the battery's performance capabilities. If the battery SOH is poor, the battery may not provide the power needed for proper vehicle operation. Battery SOH can serve as a critical indication of the need to replace or service the battery to maintain safe vehicle operation. This can be quantified in terms of the battery capacity or power, as given in Eq. (7). As the battery ages, irreversible losses in the battery reduce the active material and the amount of charge that can be stored. Also, the battery's internal resistance increases over time which results in a reduction of the power delivered by the battery. Battery SOH is measured relative to the beginning of life conditions of the battery. Here, we use capacity as a measure of SOH.

As stated above, the battery capacity is difficult to identify precisely. This is due to the dependency of battery capacity on temperature, C-rate, and battery condition. For the purposes of this work, the capacity will be assumed constant and known since operating conditions will be controlled and variations in capacity are expected to be minimal.

$$\mathrm{SOH} = {}^{\mathrm{Capacity_t}}/_{\mathrm{Capacity_0}}$$
$$\mathrm{SOH} = {}^{\mathrm{Power_t}}/_{\mathrm{Power_0}} \qquad (7)$$

Although SOC and SOH are relatively simple concepts, it is very difficult to quantify these values with certainty during vehicle operation. SOC and SOH are battery states which are not directly or easily measureable and also vary dynamically with battery operating conditions. Estimation algorithms utilize battery models and measured data to estimate the battery states and parameters.

Estimation Algorithm

There are a number of techniques that can be used to estimate the states of systems [8, 9, 10, 11, 12, 13, 14]. Estimation techniques utilize measured data as inputs to the model and outputs estimated values for the parameters and states of the model. The model simulates the dynamics of the real process, called the plant. The error between the plant and the model can be a result of the inaccuracy of the model or due to the parameters.

Assuming that the model is representative of the plant dynamics, the estimator adjusts the model states and parameters to minimize the error between the plant and the model. In this way, the hidden states and parameters can be estimated.

The estimator used in this paper is the Kalman Filter (KF). The KF is a linear estimator that employs the algorithm described below:

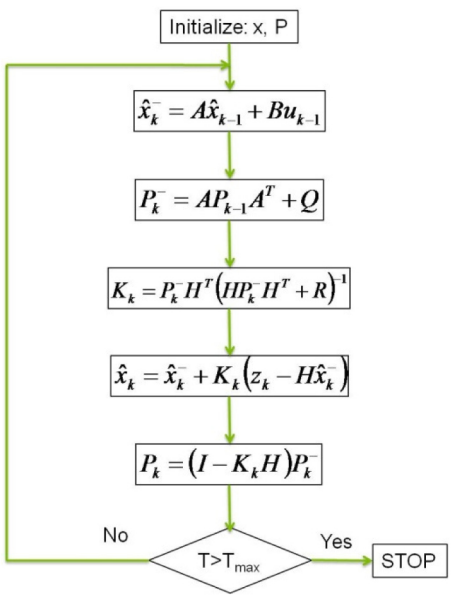

Figure 4. Flow chart of algorithm.

The algorithm is initialized at T = 0 with the initial values for the states and parameters. The initial covariance matrix, P, is defined as I_{nxn}, where n is the total number of states and parameters in the state vector, x. For each time step, a prediction and correction step are performed. The prediction step makes an estimation on the next state values based on the transition function. The covariance matrix is also updated and incorporates the process noise values. The correction step utilizes the error between the measured plant value and the estimated model value using the Kalman gain, K.

The Kalman Filter uses the gain and measured signal to correct the battery estimation and covariance matrix. The corrected estimate is stored and the algorithm iterates to the next time step. The KF is applied online using the model and measured battery current, battery temperature, and time. The algorithm's primary function is to estimate the battery SOC.

The KF has advantages and disadvantages. The KF is very simple to implement and does not require much computational power. However, the KF is a linear estimator and does not function well if the model is inherently nonlinear or if the states are nonlinear. Although this poses a limitation to the nonlinear behavior of the battery, the SOC of the lead-acid battery is a semi-linear function of OCV and changes slowly over time. Also, the battery model assumes

that the battery and parameters behave linearly as well. It is understood that this will limit the accuracy of the estimates and other advanced algorithms can be explored to provide more accurate estimation.

Start-Stop Drive Cycle

Vehicle fuel economy can vary depending on the drive cycle. For start-stop applications, the optimal drive cycles are urban-based profiles where there are numerous and long stop events, stop lights or high traffic with long idle events. In these cases, the drive cycle impact the battery substantially. During long stop events, the battery will support the vehicle electronics, causing the SOC to deplete. The battery SOC will need to be replenished, which opens the opportunity to apply alternate charging strategies. This will require an accurate estimation of the battery SOC to minimize inefficiencies during charging.

Depending on the battery SOC and the Coulombic efficiency during charging conditions, it may be possible to apply different charging voltages. At low SOC, it may be possible to quickly charge the battery at higher voltages without much loss due to gassing. At higher SOC, the charging voltage can be set lower to minimize gassing.

In this work, the FTP drive cycle, shown in Figure 5, will be used to assess the model and estimation algorithm under a start stop application. In this situation, the battery experiences high charge loads due to regenerative braking events. In addition, the battery will experience high discharge loads due to cranking events following a stop event.

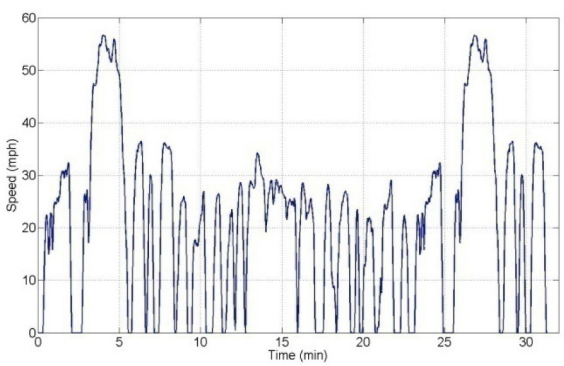

Figure 5. FTP drive cycle profile.

RESULTS

Baseline Results

The battery model and SOC algorithm was tested against standard current integration methods, as described by Eq. (7). The baseline data included battery data generated under laboratory conditions.

The battery used to validate the model and algorithm is an Absorbent Glass Mat (AGM) 95 Ah battery. The baseline data included constant current charge and discharge current and voltage profiles, seen in Figure 6. The data was collected using battery cycler that maintained constant temperature conditions.

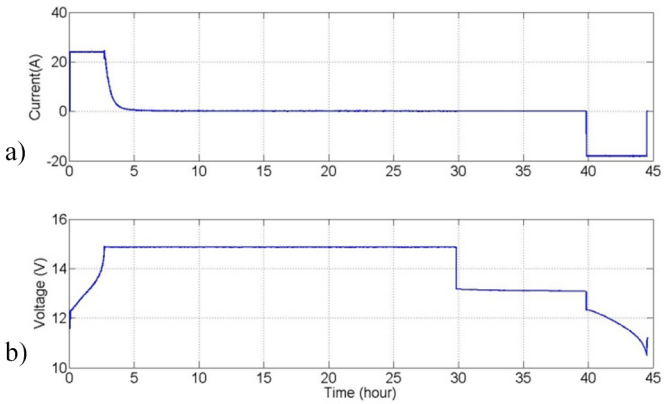

Figure 6. a) Current and b) voltage profiles.

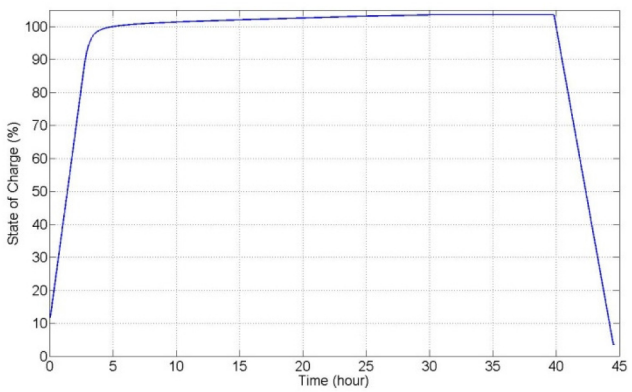

Figure 7. SOC calculated based on current integration.

The battery model and SOC algorithm are applied to the constant current charge and discharge profile. The results are compared to current integration. The integrated SOC is shown in Figure 7. As can be seen in the figure, the battery state of charge goes above 100%. Understanding that once the active material has been converted back to lead and lead dioxide, the current supplied to the battery is loss through the gassing reactions where the Coulombic efficiency is reduced to zero. This simple example illustrates the problem of using current integration to estimate the battery SOC while top charging.

The battery model and algorithm are used to estimate the battery SOC and the nonlinear voltage, V_{nl}. The results are shown in Figure 8. The measured and estimated voltages compare well. The OCV_{int} and OCV_{est} are the open circuit voltages based on SOC calculated using current integration, SOC_{int}, and SOC estimated using the algorithm, SOC_{est}. The SOC values are compared in Figure 8(c). The SOC values compare well and matches expected results.

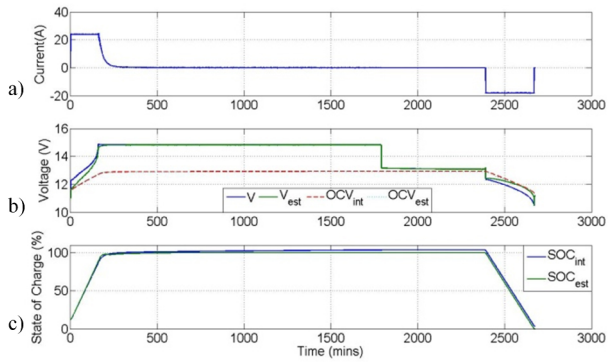

Figure 8. a) Current profile. b) compare measured and estimated terminal and open-circuit voltages. C) compare integrated and estimated SOC

Dynamic Estimation Results

The battery model and SOC algorithm were used to estimate the battery SOC using experimental battery data. The battery current and voltage profile are shown in Figure 9. The SOC is calculated using current integration. At T = 0, the battery has been rested and the battery OCV can be correlated to the SOC using calibration tables. At T = end, the battery has again been rested so that the battery OCV can be correlated to SOC.

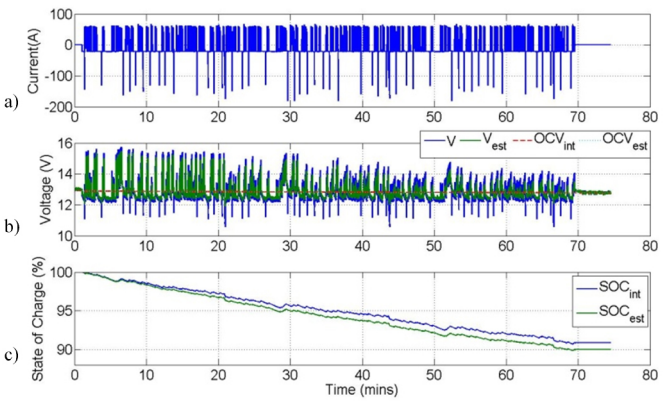

Figure 9. a) Current, b) voltages, and c) SOC values.

We can see that using current integration, there is some mismatch between the integrated SOC value and the SOC value correlated to the battery OCV. This may be due to the noise in the current. This SOC drift is a limitation to long durations of current integration.

The battery model and SOC algorithm were applied to the same battery data. The estimated battery SOC is compared to the integrated value. It can be seen that as the battery operation continues, the differential between the integrated and estimated SOC values increases. However, at T = end, we can see that the estimated SOC value correlates well to the SOC value correlated to the battery OCV.

A close-up analysis of the results are shown in Figure 10. This figure shows that the measured and estimated voltage correlate well. This indicates that the battery model is sufficient to capture the battery dynamics. The small mismatch may be reduced if a higher order model was used. This can be applied in future works. However, the battery SOC was estimated using the model and estimation algorithm discussed in this paper and correlate well to expected results.

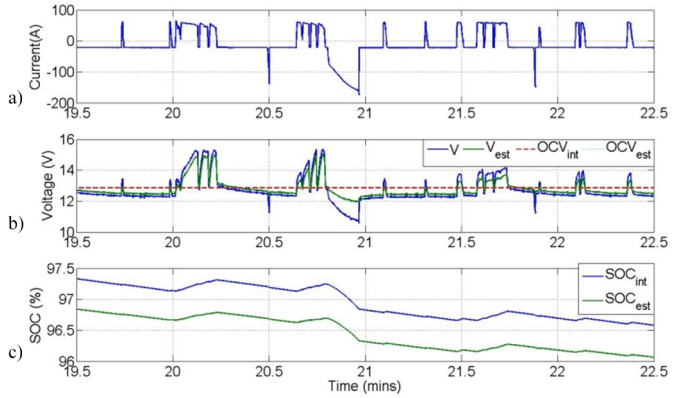

Figure 10. a) Current, b) voltages, and c) SOC values for T = [19.5 22.5] mins

SUMMARY

An equivalent circuit lead-acid battery model incorporating losses due to gassing reactions under charge was developed. A Kalman Filter was applied to estimate the battery SOC. The battery model and SOC algorithm work well to capture the battery dynamics under operation and accurately estimates the battery SOC. This research shows the importance of including gassing losses in a lead-acid battery in order to accurately represent the chemistry dynamics and accurately estimate the battery SOC. This work can be extended to include SOH estimation.

REFERENCES

1. Salameh, Z.M., Casacca, M.A., and Lynch, W.A., "A Mathematical Model for Lead-Acid Batteries," *IEEE Transactions on Energy Conversion*, 7(1):93-98, 1992.
2. Ceraolo, M., "New Dynamical Models of Lead-Acid Batteries," *IEEE Transactions on Power Systems*, 15(4):1184-1190, 2000.
3. Thele, M., Shiffer, J., Karden, E., et al., "Modeling of the charge acceptance of lead-acid batteries," *Journal of Power Sources*, 168(1): 31-39, 2007.
4. Rynkiewicz, R., "Discharge and charge modeling of lead acid batteries," presented at Applied Power Electronics Conference and Exposition, USA, March 14-18, 1999.
5. Berndt, D., "Valve Regulated Lead Acid Batteries," *Journal of Power Sources*, 100(1-2):29-46, 2001.
6. Ceraolo, M., "New Dynamical Models of Lead-Acid Batteries," *IEEE Trans. Power Systems*, 15(4): 1184-1190, 2000.
7. Larminie, J. and Lowry, J., "Electric Vehicle Technology Explained," 2nd Edition, John Wiley & Sons, West Sussex, ISBN: 978-1-1199-4273-3, 2003.
8. Welch, G., Bishop, G., "An Introduction to the Kalman Filter_Welch," TR 95-041, UNC Chapel Hill, 2006.
9. Simon, D., "Kalman Filtering with State Constraints: A Survey of Linear and Nonlinear Algorithms," *IEI Control Theory & Applications*, 4(8):1303-1318, 2009.
10. Barbarisi, O., Vasca, F., and Glielmo, L., "State of charge Kalman Filter Estimator for Automotive Batteries," *Control Engineering Practice*, 14(3):267-275, 2006.

11. Choudhury, J.R., Banerjee, T.P., Gurung, H., et al., "Real time state of charge prediction using Kalman Filter," presented at World Congress on Nature & Biologically Inspired Computing, India, Dec. 9-11, 2009.
12. Vasebi, A., Partovibakhsh, M., and Bathaee, S., "A novel combined battery model for state-of-charge estimation in lead-acid batteries based on extended Kalman filter for hybrid electric vehicle applications," *Journal of Power Sources*, 174(1):30-40, 2007.
13. Zhang, J., "State of Charge Estimation of Valve Regulated Lead Acid Battery Based on Multi State Unscented Kalman Filter," *International Journal of Electrical Power & Energy Systems*, 33(3):472-476, 2011.
14. Han, J., Kim, D., and Sunwoo, M., "State-of-charge estimation of lead-acid batteries using an adaptive extended Kalman filter," *Journal of Power Sources*, 188(2):606-612, 2009.

CONTACT INFORMATION

Dr. Daniel Le, *Staff Scientist*
Johnson Controls - Power Solutions
5757 N. Green Bay Ave, LD-67
Milwaukee, WI 53209
Daniel.Le@jci.com
Tel: 414-524-2091

DEFINITIONS/ABBREVIATIONS

OCV - Open-Circuit Voltage

$\mathbf{R_s}$ - Ohmic Resistance

$\mathbf{R_{nl}}$ - Nonlinear Resistance

$\mathbf{C_{nl}}$ - Nonlinear Capacitance

$\mathbf{I_m}$ - Main Branch Current

$\mathbf{I_g}$ - Gassing Branch Current

$\mathbf{I_t}$ - Terminal Current

$\mathbf{V_t}$ - Terminal Voltage

$\mathbf{V_g}$ - Gassing Voltage

H - Coulombic Efficiency

$\hat{\boldsymbol{x}}^-$ - *a priori* state estimate

$\hat{\boldsymbol{x}}$ - *a posteriori* state estimate

$\hat{\boldsymbol{P}}^-$ - *a priori* covariance estimate

$\hat{\boldsymbol{P}}$ - *a posteriori* state estimate

K - Kalman gain

$\mathbf{z_k}$ - Measurement value

$\mathbf{u_k}$ - Input value

Q,R - Process and Observation Noise Covariance